



Change of pore size in concrete due to electrochemical chloride extraction and possible implications for the migration of ions

Michael Siegwart^{a,*}, John F. Lyness^{b,1}, Brian J. McFarland^c

^a*FaberMaunsell Ltd., Imperial House, 31 Temple Street, Birmingham B2 5DB, UK*

^b*School of the Built Environment, University of Ulster, Newtownabbey BT 37 0QB, Northern Ireland, UK*

^c*McFarland Associates, Ormsdale 375, Upper Newtownards Road, Belfast BT4 3LF, UK*

Received 31 May 2002; accepted 21 January 2003

Abstract

Electrochemical chloride extraction (ECE) is used for the rehabilitation of chloride-contaminated concrete. Anions such as chloride and hydroxide are pushed away from the cathode (reinforcement), and cations such as sodium, potassium and calcium are attracted to the cathode. During ECE an increase of the concrete resistance can be observed. The results of a petrography study on ECE-treated concrete are presented in this paper. It also investigates the influence of pore size on ion migration using a concrete substitute model with known pore size. Findings showed that the pore size and pore size distribution of concrete are altered due to ECE. It is therefore suggested that concrete acts as active migration medium in the migration process by releasing ions into the pore solution. Moreover, small pores hinder the migration of ions, which may partially be responsible for changes in concrete resistance.

© 2003 Elsevier Science Ltd. All rights reserved.

Keywords: Microstructure; Pore size distribution; Electrochemical properties; Chloride; Concrete

1. Introduction

The main causes of reinforcement corrosion are chlorides and carbonated concrete. Electrochemical chloride extraction (ECE) and its sister technique, realkalisation, are used to restore chloride-contaminated or carbonated concrete. The advantage of these processes is the migration of ions (rehabilitation) under an electrical field in concrete that is much faster than their diffusion (contamination). The chloride contamination through diffusion can thus be reversed in a short period of time. Migration and diffusion of charged species, such as chloride in concrete, depend on several factors related to its pore structure, which is altered during ECE.

2. Ion migration and electrical field strength

It has been suggested that ion transport through cement-based material can properly be described only by using a combination of the processes of Nernst–Planck and the electrical double layer diffusion processes [1]. Using the Nernst–Planck equation, the migration of ions may be obtained as follows:

$$\frac{\partial C_i}{\partial t} = D_i \frac{\partial^2 C_i}{\partial x^2} + D_i \frac{\partial C_i}{\partial x} t_i E \frac{zF}{R_G T} \quad (1)$$

where C is the concentration of the ion i , t the time, D the diffusion coefficient, t_i the transport number, F is Faraday's constant, z the valence of the ion, R_G the gas constant, x the location, E the electrical field strength and T the temperature.

The ions in the pore water transport electrical current; thus, resistivity is a measure of the continuity of the pore solution through which chlorides migrate [2,3]. The concrete resistivity is an indication of its chloride permeability [4,5]. Dry concrete acts as electrical insulator and its resistivity is approximately 109 Ω m. In contrast, moist

* Corresponding author.

E-mail addresses: michael.siegwart@fabermaunsell.com (M. Siegwart), jf.lyness@ulster.ac.uk (J.F. Lyness), mcfass@ntlworld.com (B.J. McFarland).

¹ Tel.: +44-2890-366506; fax: +44-2890-366826.

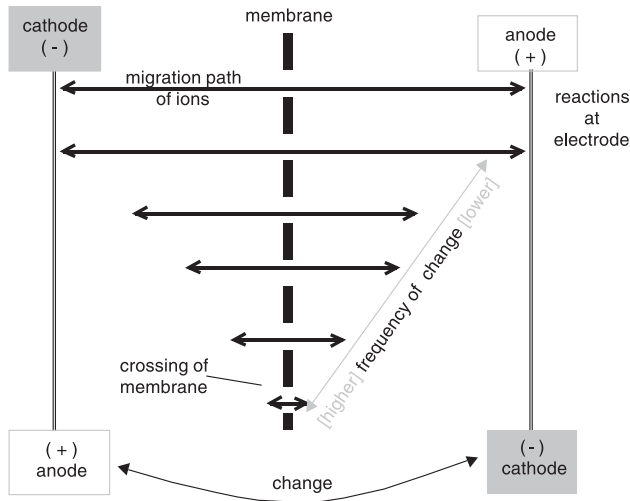


Fig. 1. Migration path of ions through membrane during impedance spectroscopy measurements.

concrete acts as conductor with a resistivity of approximately 50 Ω m [6].

Hassanein et al. [7] proposed that resistivity can be obtained by dividing the IR voltage drop across the specimen by the average current density and the specimen thickness. Other authors obtained the chloride diffusivity in concrete from its resistivity [8]. The resistivity of silica fume blended cement is higher compared to plain ordinary portland cement because of smaller pores [9] and, for the same reason, carbonation increases the electrical resistivity and water adsorption of concrete [10]. Resistivity and resistance (*R*) are related as follows [11]:

$$\rho = \frac{RA}{\lambda} \quad (2)$$

where ρ is the resistivity, *A* the electrode area, λ the distance between the electrodes and *R* the resistance. However, it is difficult to obtain the true resistivity of concrete using nondestructive techniques, as concrete is an inhomogeneous material [12]. The resistivity obtained from such a material does not follow Eq. (2) and is an apparent resistivity value, which depends on the electrode configurations [13]. Moreover, the area of the cathode and anode vary in practical applications of ECE, where the cathode is a reinforcement

Table 1
Mix proportions of prestressed concrete

Component	Mass [kg]
Mixing water	182.00
Cement CE 42.5	460.00
W/c ratio	0.40
Sand	755.00
Fine aggregate (size < 10 mm)	391.00
Coarse aggregate (size < 20 mm)	586.00
Sodium chloride	11.37

Table 2
Compressive strength of prestressed concrete

Temperature cured (at 105 °C)	Ambient temperature (at 20 °C)	Control (chloride-free)	Chloride control (1.2 wt.% chloride)
3/2325/36.0 ^a	3/2361/29.4	N.A.	N.A.
3/2326/36.1	3/2336/29.5		
3/2349/33.1	3/2347/26.8		
3/2295/35.5	3/2390/33.1		
Average: 35.2 N/mm ²	Average: 29.7 N/mm ²	–	–
28/2314/49.6	28/2371/52.8	28/2438/60.5	28/2385/52.5
28/2302/48.0	28/2332/55.7	28/2383/61.0	28/2442/51.0
28/2316/46.7	28/2392/51.8	28/2432/59.2	28/2337/54.2
28/2378/47.1	28/2347/47.1		
28/2321/48.8	28/2319/50.6		
Average: 48.0 N/mm ²	Average: 51.6 N/mm ²	Average: 60.2 N/mm ²	Average: 52.5 N/mm ²

^a Test age [days]/weight [g]/compressive strength [N/mm²].

bar and the anode a titanium mesh. Resistance can be obtained according to Ohm's law as follows:

$$R = \frac{V}{I} \quad (3)$$

where *V* is the potential and *I* the current. It has been shown that the resistivity of concrete is related to the resistance of the system. The resistivity determines the electrical field strength governing the extraction efficiency during ECE (Eq. (1)), which can be obtained from the concrete resistivity as follows:

$$E = \rho J \quad (4)$$

where *J* is the current density and *E* is the electrical field strength. Therefore, it is clear that increasing resistivity raises the electrical field strength. The diffusivity of ions in concrete relates to the tortuosity. Increased diffusion path length reduces the diffusivity of ions in concrete compared to ions in free solutions.

Although high concrete resistivity is required to simulate migration of ions, it cannot be tortuosity induced as the tortuous path length will reduce the resistivity (Eq. (2)) and, therefore, the electrical field strength.

3. Background on impedance spectroscopy

Impedance spectroscopy is used to measure the changing properties of an electrolytic cell. A current or potential perturbation at varying frequencies is passed through the cell. The electrical resistance of the system reflects the

Table 3
Chemical composition of cement (%)

SiO ₂	Al ₂ O ₃	Fe ₂ O ₃	CaO	MgO	SO ₃	Na ₂ O	K ₂ O	Na ₂ O	Cl
20.53	5.07	3.24	63.85	2.45	3.09	0.1	0.55	0.46	0.028

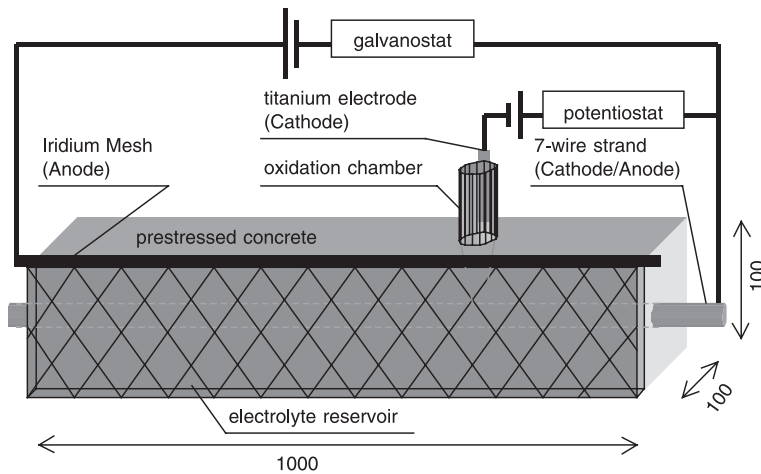


Fig. 2. Experimental set-up of prestressed concrete with a seven-wire strand.

reactions of an electrode system. The total resistance or impedance (Z) is obtained from the forces that resist ion migration in the solution (R_s), the double layer formed on the electrodes depending on the applied frequency (f) and the capacitance of the electrode (C_{cap}) [14]. The impedance at low frequencies incorporates reaction of the ions on the surface of the electrode such as the formation of a double layer. The capacitance is constant, but the resistance of the solution and the double layer depend on the concentration of ions. The impedance for any frequency (f) can be obtained as follows:

$$Z = R_s + \frac{1}{jC_{cap}2\pi f} \quad (5)$$

As ions do not react on the surface of the electrode, the resistance of the system at high frequencies approximates R_s and can be calculated following Ohm's law:

$$R = Z = \frac{V}{I} \quad (6)$$

It is not possible to obtain concrete or cement paste with uniform pore size, and thus an alternative material has to be

used to measure the effect of pore size on ion migration. The thickness of the filter membrane selected for this study was a few micrometres, whereas that of the concrete cover is some centimetres. Using impedance spectroscopy measurements, one thin membrane can represent concrete, as the migration of species is reversed at high frequencies. The membrane in this case has the same effect with concrete (Fig. 1). Other effects such as interactions with ions on pore walls, the double layer diffusion [15] and chloride binding do not take place, as the membrane is electroneutral.

4. Research significance

It has been assumed that the change of concrete pore size and pore size distribution is a side effect of the migration process. It has not been considered before how these two factors could influence the migration process, but this study provides a new perspective to the phenomenon of ion migration in concrete by exploring the influence of the reduced pore size on the migration of ions in concrete.

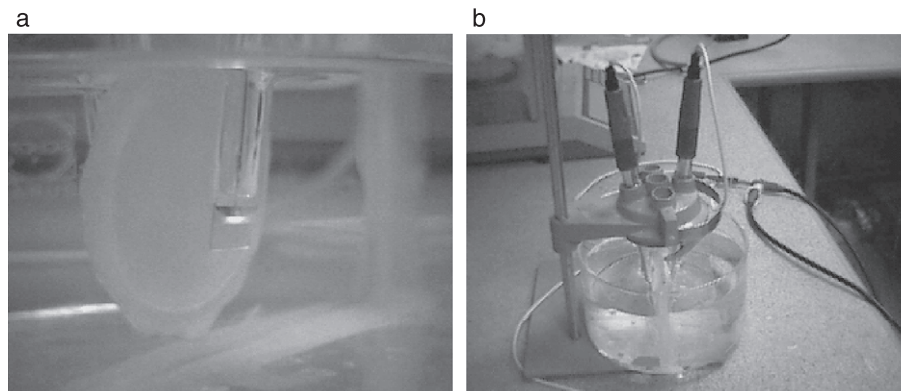


Fig. 3. Membrane in Perspex barrier (a) and experimental set-up (b).

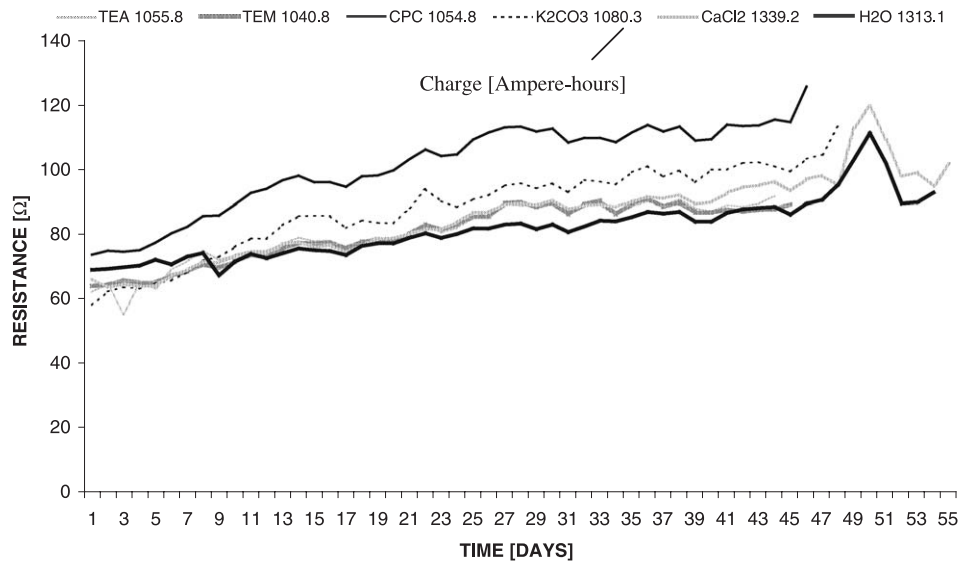


Fig. 4. Resistance of concrete samples with different electrolytes during ECE.

The findings suggest that concrete acts as an active migration medium rather than as a passive background to ion migration.

5. Experimental programme

The experimental programme comprised two parts, the petrography analysis of ECE-treated concrete and the impedance spectroscopy on a concrete substitute material containing artificial concrete pore water. The composition of concrete pore water and the range of concentrations of individual species can be reproduced for laboratory investigation [16].

The mix proportion of the concrete used for the six specimens is given in Table 1. The concrete was heat cured because it contained prestressed steel. In addition, temperature control samples were cast to assess the effects of heat curing on porosity and compressive strength, which was

tested at 3 days and at 28 days (Table 2). The chemical composition of the cement is shown in Table 3.

The concrete specimens were subjected to ECE treatment for a period of 40 days; the experimental set-up is depicted in Fig. 2. The treatment was monitored using a computerised, data-logging system in which the current and potential readings were taken every 100 s. Ordinary tap water was used as an electrolyte in this study. Other samples were tested in parallel and contained different chemicals to test their migration properties in concrete [17]. The chemicals were tetraethylammonium iodide, tetramethylammonium chloride, cethylpyridinium chloride, potassium carbonate and calcium chloride. Their purpose was to suppress the hydrogen uptake on the steel surface and mitigate hydrogen embrittlement. However, they did not reach the steel surface, and therefore hydrogen was taken up by the steel.

The concrete pore size and the pore size distribution of the concrete sample containing the tap water electrolyte (H₂O) were analysed after the ECE treatment at various

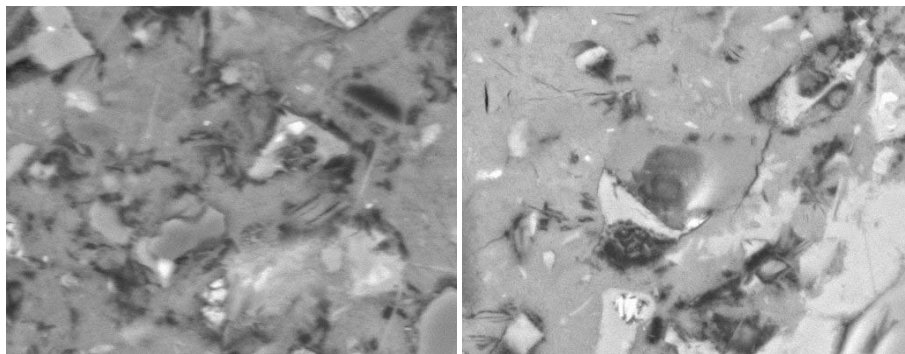


Fig. 5. SEM images taken from untreated concrete (Control Area 1 with 218 pores at $0.85 \pm 0.09 \mu\text{m}$ and Area 3 with 169 pores at $0.62 \pm 0.09 \mu\text{m}$, average \pm S.D.).

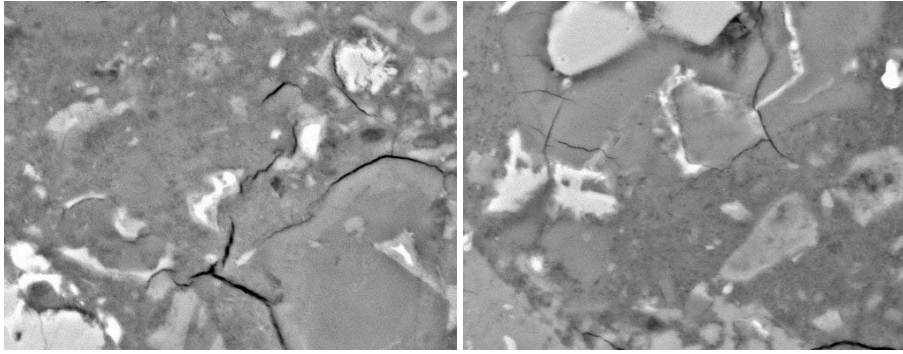


Fig. 6. SEM images taken from ECE-treated concrete at a distance of 3 mm from the reinforcement impression (Surface 1 Area 2 with 414 pores at $0.33 \pm 0.05 \mu\text{m}$ and Area 5 with 443 pores at $0.30 \pm 0.04 \mu\text{m}$, average \pm S.D.).

depths and compared to an untreated control. Samples were sliced and impregnated with an epoxy resin. The untreated control sample was sliced in the middle, whereas the ECE-treated sample was cut at 3, 16, 29 and 42 mm from the reinforcement (prestressing strand) impression.

The hardened surfaces were polished and scanning electron microscopy (SEM) images were taken at eight different locations on each surface. The magnification was $\times 2000$, representing an area of $64 \times 50 \mu\text{m}$. The images

were analysed using the Oxford Systems ISIS 300 System IMQuant Software to obtain the pore size and pore size distribution of each image.

The diffusion and migration of ions in concrete is a complex interaction of various factors such as concentration of migrating species in different layers of the concrete, physical properties of the concrete and binding processes. Thus, it is not possible to investigate the influence of one single parameter on ion migration using concrete.

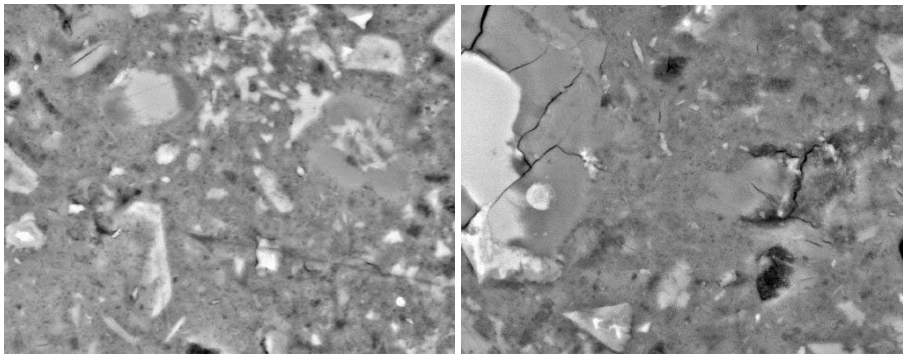


Fig. 7. SEM images taken from ECE-treated concrete at a distance of 16 mm from the reinforcement impression (Surface 2 Area 2 with 1011 pores at $0.37 \pm 0.05 \mu\text{m}$ and Area 4 with 598 pores at $0.41 \pm 0.06 \mu\text{m}$, average \pm S.D.).

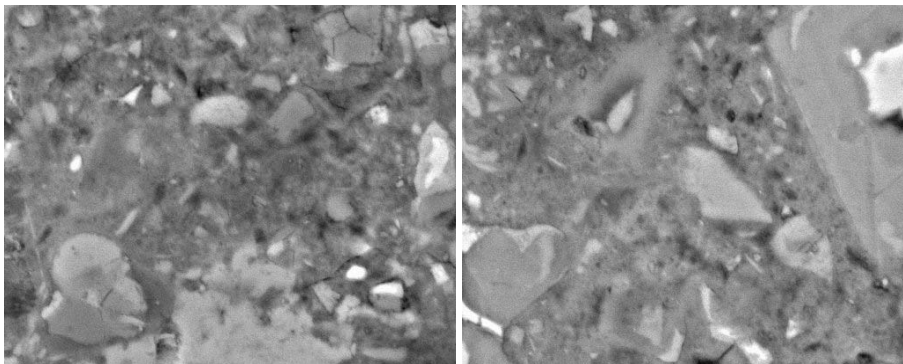


Fig. 8. SEM images taken from ECE-treated concrete at a distance of 29 mm from the reinforcement impression (Surface 3 Area 3 with 572 pores at $0.37 \pm 0.05 \mu\text{m}$ and Area 4 with 497 pores at $0.37 \pm 0.05 \mu\text{m}$, average \pm S.D.).

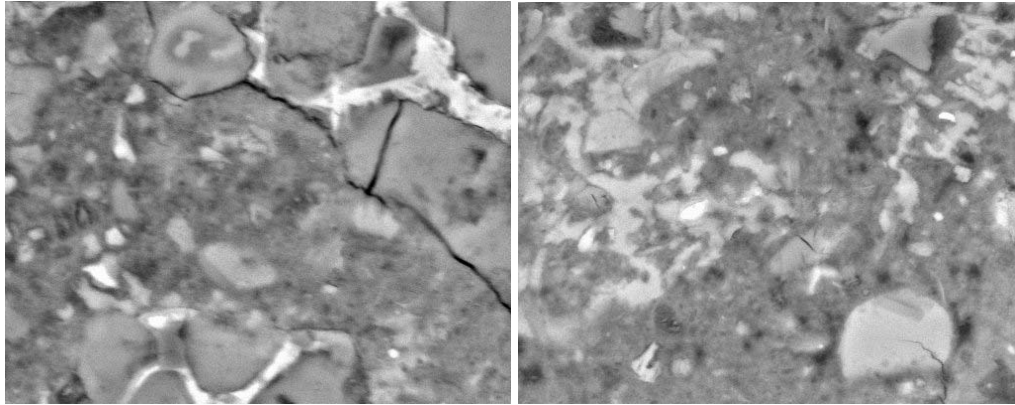


Fig. 9. SEM images taken from ECE-treated concrete at a distance of 42 mm from the reinforcement impression (Surface 4 Area 1 with 350 pores at $0.46 \pm 0.06 \mu\text{m}$ and Area 3 with 265 pores at $0.50 \pm 0.06 \mu\text{m}$, average \pm S.D.).

The pore size of concrete and cement paste is between 0.003 and $1.000 \mu\text{m}$ for young cement pastes and between 0.003 and $0.1 \mu\text{m}$ for mature cement pastes [18]. Instead of concrete, a material with known pore size, Whatman Anopore filter membranes with 0.02 , 0.10 and $0.20\text{-}\mu\text{m}$ pore diameter were used to investigate the influence of pore size on migration.

The experimental set-up is depicted in Fig. 3. An impermeable Perspex membrane with a 35-mm \emptyset hole in the centre was glued into a crystallisation dish to form two compartments. The hole was sealed with a permeable filter membrane, thus making the migration of ions possible only through the membrane. Two platinum electrodes with an electrode area of 1 cm^2 were placed at a 2-cm distance of each other, separated either by the membrane or the plain solution in case of measurements without the membrane.

The impedance measurements of the influence of pore size of membranes in artificial concrete pore solution were conducted with a Schlumberger SI 1260 Impedance/Gain Phase Analyser and SI 1286 Electrochemical Interface.

6. Experimental results

The ECE treatment was carried out for 1000 h with a current density of $1.00 \text{ Ampere per square metre}$ of steel surface ($0.66 \text{ Ampere per square metre}$ of concrete surface). The concrete was aged 3 months at the time of the ECE

treatment. The development of the resistance of the samples is depicted in Fig. 4.

It was found that the pore size and pore distribution had changed due to ECE. A visual examination of the image areas revealed differences in the pore size distribution between the control sample and the four surfaces taken from the treated sample. The pores in the control sample occurred less frequently and were larger than those in the treated sample (Figs. 5–9).

The effects of ECE treatment on pore size and pore size distribution for different samples are summarised in Table 4. It shows a summary of the results obtained from the analysis of eight scanning electron microscope images from each concrete surface. The data obtained from these images were analysed collectively. This is contrast to the values shown in the labels of Figs. 5–9, which were obtained from the analysis of the individual images. The control sample contained considerably fewer pores and generally larger pores than those in the treated sample. The total number of pores in the treated sample was the lowest in the S4 surface, which was in proximity of the anode. The petrography analysis showed that ECE treatment changes the pore structure of concrete. These findings are consistent with those reported by Banfill [19].

Table 5 shows the composition of the solutions used for the impedance spectroscopy. Similar results were obtained for all solutions, and for this reason only the impedance measurement of the calcium hydroxide solution through the $0.02\text{-}\mu\text{m}$ membrane is depicted in Fig. 10.

Table 4
Pore size and pore size distribution in concrete due to ECE treatment

Surface (at x mm from reinforcement impression)	Number of pores	Average pore size (μm)	S.D. (μm)
Control	1479	0.70	± 0.10
1 (at 3 mm)	4296	0.35	± 0.05
2 (at 16 mm)	4463	0.39	± 0.05
3 (at 29 mm)	3528	0.39	± 0.06
4 (at 42 mm)	2309	0.47	± 0.06

Table 5
Concentration of ions for impedance spectroscopy

Name (chemical abbreviation)	Concentration [g/l]
Potassium hydroxide (KOH)	2.0
Sodium hydroxide (NaOH)	0.3
Calcium hydroxide ($\text{Ca}(\text{OH})_2$)	0.1
Sodium chloride (NaCl)	2.5
Artificial concrete pore water	Sum of above components

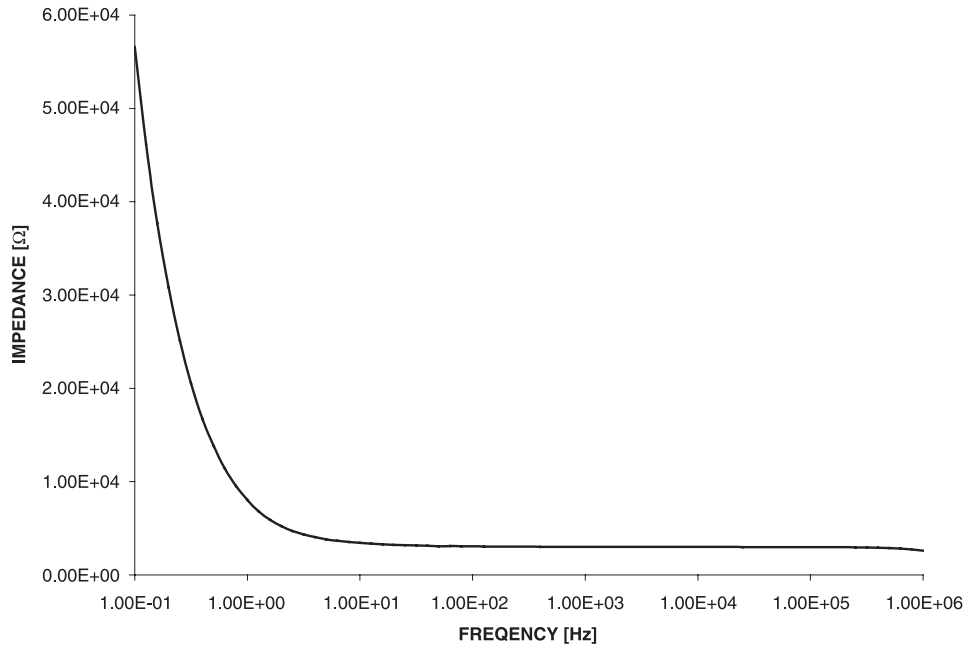


Fig. 10. Results of impedance measurement of calcium hydroxide solution through a 0.02- μm membrane.

Direct current is used during ECE compared to the alternating current regime used during impedance spectroscopy. For this reason, some experiments on the membrane system were conducted under a direct current regime. The results of the measurements on the 0.02- μm membrane using artificial pore water are shown in Fig. 11. As a wide scatter of results were obtained compared to impedance spectroscopy, the DC measurements were not analysed further. The experimental scatter can be explained by

electrode reactions such as hydrogen formation and the adsorption of ions at the electrodes.

7. Analysis and discussion of results

The results of the impedance spectroscopy showed an increase in resistance when the membrane was placed between the electrodes for different electrolytes. This effect

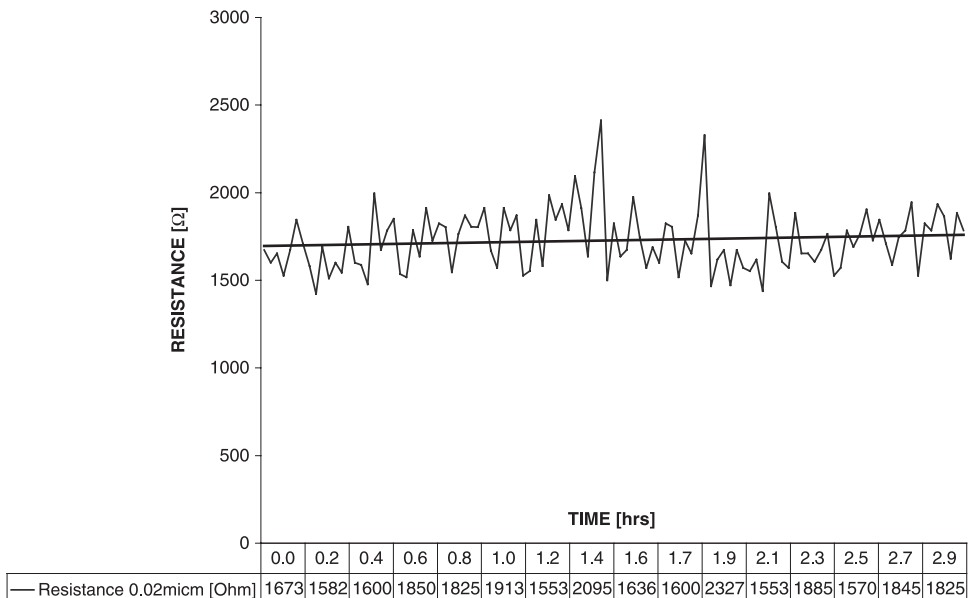


Fig. 11. Resistance of a 0.02- μm membrane under DC regime.

was observed at both low and high frequencies, although the resistance increased significantly below a certain frequency. This can be attributed to the build-up of a double layer and the occupation of free sites on the two electrode surfaces by the adsorption and subsequent reactions of ions.

This effect is even more significant during ECE when a direct current is applied. This results in an instantaneous formation of a reactive layer on the electrode surface with a corresponding increase in resistance. It can then be concluded that resistance measurements under a direct current source always contain errors due to the build-up of the double layer and do not truly reflect the migration properties of ions in the concrete.

Concrete could act as a membrane [20] and due to the build-up of a concentration gradient across the membrane, i.e., between the reinforcement and the anode, a potential gradient would develop caused by the nonuniform distribution of charged species. This potential is called the membrane potential and contributes to the increase of the resistance. This effect cannot be confirmed directly due to the wide experimental scatter of the DC measurements (Fig. 11).

However, in the present study, electroosmosis was observed during DC measurements on the Anopore membrane system. The quantity of the anolyte increased by approximately 20% while the quantity of the catholyte decreased by an equal amount. Electroosmosis has also been observed using a concrete membrane [21]. This effect occurs because the migration of cations is faster than that of anions. Anions and cations are dissolved and surrounded by water molecules that migrate with them. This water then accumulates in the catholyte. A separation of charge and, subsequently, a membrane potential occurs for this set-up. However, this effect does not occur during ECE [22]. Concrete is a porous material. It has been argued that porous materials are used in fuel cells in order to increase their efficiency by preventing the build-up of membrane potentials [23].

Two effects were observed on the Anopore membranes; first, the initial resistance of the system was different due to different pore size of the membranes and second, with lower frequency, the resistance increases slightly. The line parallel to the horizontal in Fig. 10 represents R_s , but during ECE, electrode processes occur. Therefore, the average resistance of all frequency ranges were used for the analysis of the effect of pore size on ion migration (Table 6).

It can be seen in Fig. 12 that the percentage increase in resistance of the different solutions is plotted against the pore sizes. The resistance of the solution without membrane was assumed to be equal to 100%. It is obvious that with the decrease of pore size, the resistance of the artificial pore solution and the calcium hydroxide increases, thus indicating a linear relationship between them. A logarithmic relationship gives a good approximation of

Table 6
Results of impedance spectroscopy measurements

Frequency range (Hz)	Solution	Impedance (Ω)	Pore size of membranes (μm)			Free migration ($>\mu\text{m}$)
			0.02	0.10	0.20	
	NaOH		0.02	0.10	0.20	10.00
10^6			3313	3289	3279	3180
$10^6-3\times 10^3$			4017 ^a	3945 ^a	3940 ^a	3668 ^a
10^6-10^{-1}			7641 ^b	7491 ^b	7383 ^b	7007 ^b
	NaCl		0.02	0.10	0.20	4.00
10^6			4384	4411	4523	4450
$10^6-3\times 10^3$			5955 ^a	5874 ^a	5921 ^a	5675 ^a
10^6-10^{-1}			10,456 ^b	10,234 ^b	10,086 ^b	9666 ^b
	KOH		0.02	0.10	0.20	1.00
10^6			3760	3546	3589	3434
$10^6-3\times 10^3$			4731 ^a	4330 ^a	4295 ^a	3975 ^a
10^6-10^{-1}			8444 ^b	8038 ^b	7959 ^b	7618 ^b
	CaOH ₂		0.02	0.10	0.20	6.48
10^6			2591	2597	2565	2371
$10^6-3\times 10^3$			3018 ^a	2993 ^a	2972 ^a	2580 ^a
10^6-10^{-1}			6653 ^b	6549 ^b	6467 ^b	6033 ^b
	Artificial pore solution		0.02	0.10	0.20	10.41
10^6			1411	1423	1433	1392
$10^6-3\times 10^3$			1528 ^a	1540 ^a	1548 ^a	1487 ^a
10^6-10^{-1}			6292 ^b	6249 ^b	6183 ^b	5826 ^b

^a Parallel to the horizontal.

^b Used for analysis.

the influence of pore size on resistance for the remaining three solutions.

The resistance measurements are based on four points on the vertical. However, only values for three points at the horizontal, i.e., the membrane size, are known. This was due to the absence of a membrane for the measurements in plain solutions. To find the pore size where migration remains unhindered, the relationships presented in Fig. 12 have to be extrapolated to reach the horizontal or the resistance of the system without membrane.

The results of this analysis are shown in Figs. 13 and 14. The resistance is not affected for a pore size larger than 4 μm for sodium chloride and larger than 10 μm for sodium hydroxide. It is not possible to isolate one type of ion and investigate its influence because cations are always accompanied by anions to satisfy the electroneutrality condition. However, it is possible to change one of the ions in an ion pair and the measure the effect. The coupled migration of sodium and hydroxide requires more space than the coupled migration of sodium and chloride.

Data are plotted on a normal scale in Fig. 13, and they are plotted on a logarithmic scale in Fig. 14. From the appearance of Fig. 13, it appears that the logarithmic relationship approximates better to the known values of pore sizes.

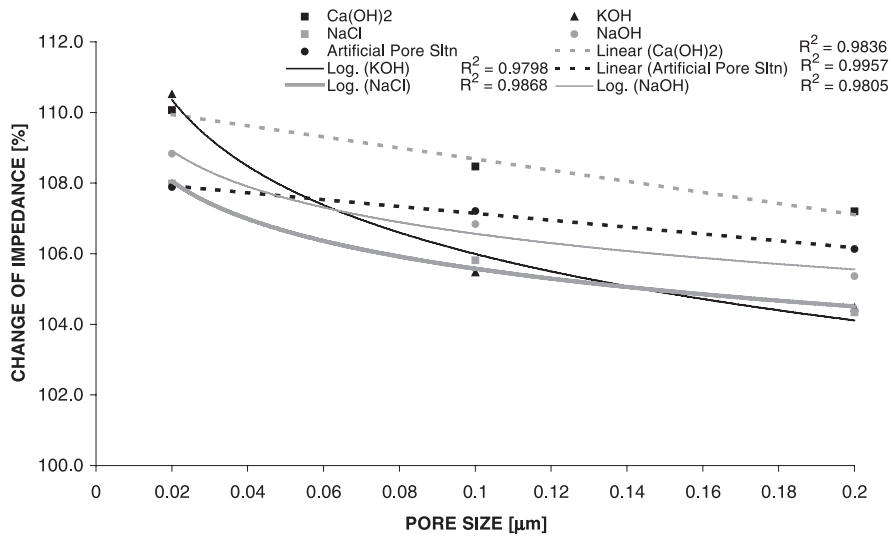


Fig. 12. Influence of pore size on impedance using different solutions (Table 5).

The logarithmic relationship cannot be used to find the minimum pore size, as it would give unrealistic high values for minimum pore sizes (100 μm for calcium hydroxide and 1000 μm for pore solution). The linear relationship, however, converges faster to the resistance without membrane and is therefore better suited to find the minimum pore size for unhindered migration.

When the linear relationship is used for extrapolation, a minimum pore size of 10.41 μm for calcium hydroxide and 6.48 μm for plain pore solution is obtained. Potassium hydroxide can migrate undisturbed through 1 μm. In contrast, calcium hydroxide requires a significantly wider space although its concentration was less than that of the potassium hydroxide (Fig. 14). The pore size of mature cement is at least 10 times less than the minimum pore size required for the

unhindered migration of potassium hydroxide. Therefore, the pore size of cement is one of the factors that hinders the migration of ions in concrete compared to free solution.

The diffusion of charged species, such as chloride and hydroxide and their corresponding cations, are related to their electrical properties as well as their interactions with the diffusive medium and with each other. The pore size and distribution changes during ECE. Amongst other factors, the change in pore size, which falls below a certain limit, influences the migration properties of the species and influences in turn, the resistance of the system. This limit is different for different ions and varies with varying concentration.

The influence of changing pore size during the application of an electrical field to concrete for migration of ions

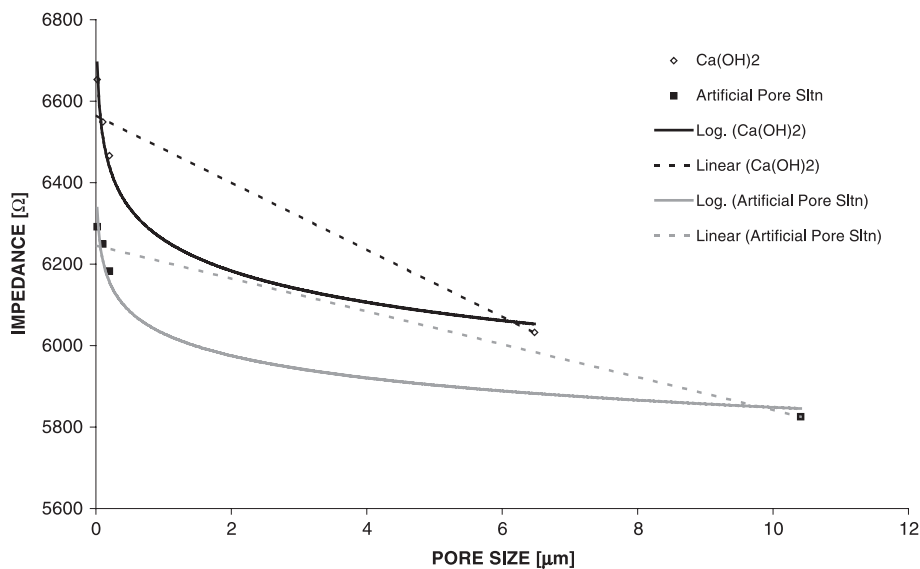


Fig. 13. Interpolated relationship between impedance range (10^6 – 10^{-1} Hz) and pore size of artificial pore solution and of calcium hydroxide solution [Ca(OH)₂]; concentrations given in Table 5.

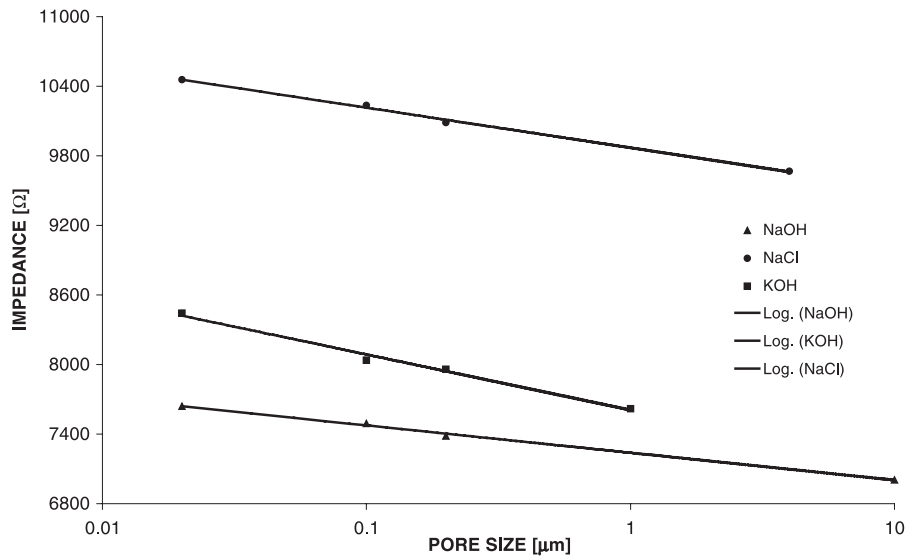


Fig. 14. Interpolated relationship between impedance range ($10^6 - 10^{-1}$ Hz) and pore size of potassium and sodium hydroxide and sodium chloride solution; concentrations given in Table 5.

can be incorporated by introducing a correction factor into Eq. (1). However, migration in concrete appears to be related to more parameters than the change in pore size. The Anopore membrane cannot account for chloride binding, which takes place in concrete. Moreover, most of the crystals forming the concrete pore structure are not electro-neutral, and therefore strong electrochemical interactions of the cement with the ions in solutions, such as the formation of double layers along pore walls [24], take place during ion migration.

The results of the petrography analysis showed that a higher number of pores with a smaller pore size appear in ECE-treated concrete compared to untreated concrete. Different pore size distribution is the result of concrete acting as an active migration medium, which modifies its pore structure through the release of ions into the pore solution during ECE.

8. Conclusions

This paper was presented the investigation of the influence of ECE on the pore structure of concrete using petrography analysis and the isolated effect of pore size on ion migration using a concrete replacement material. The following conclusions can be drawn from the present study:

1. Visual examination of the image areas and computational analysis showed obvious differences in the pore size distribution between the control sample and the four surfaces taken from the treated sample.
2. The pores in the control sample were less frequent and larger than those in the treated sample.
3. The surface close to the anode in the treated sample had the lowest total number of pores.

4. The change in pore size influences the migration properties of ions below a certain diameter, and thus influences the resistance of the system.
5. The limiting diameter for unhindered migration is different for different ions and compounds such as sodium chloride or hydroxide. Furthermore, it varies with varying concentration of ions.
6. Mature cement paste and concrete have pore sizes at least 10 times below this limit, and therefore pore size contributes to the higher resistance of ions in concrete compared to free solutions.
7. Complex interactions of the concrete with the migrating ions, such as chloride binding or the formation of double layers along the pore walls, do not allow to quantify the influence of changing pore diameter separately.

Acknowledgements

The first author would like to acknowledge the help of Dr. A. Richardot from the Northern Ireland Bio-Engineering Centre (NIBEC) for his assistance during the impedance measurements and Mr. Gareth Doyle, Structural Repair Manager, Graham Ltd., for the provision of the concrete samples.

References

- [1] S. Chatterji, Transportation of ions through cement based materials. Part 3 Experimental evidence for the basic equations and some important deductions, *Cem. Concr. Res.* 24 (7) (1994) 1229–1236.
- [2] R.F. Feldman, G.W. Chan, R.J. Brousseau, P.J. Tumidajski, Investigation of the rapid chloride permeability test, *ACI Mater. J.* 91 (2) (1994) 246–255.

- [3] R.F. Feldman, L.R. Prudencio, G.W. Chan, Rapid chloride permeability test on blended cement and other concretes: correlations between charge, initial current and conductivity, *Constr. Build. Mater.* 13 (3) (1999) 149–154.
- [4] C. Andrade, Calculation of chloride diffusion coefficients in concrete from ionic migration measurements, *Cem. Concr. Res.* 23 (3) (1993) 724–742.
- [5] P.B. Bamforth, The derivation of input data for modelling chloride ingress from eight-year UK coastal exposure trials, *Mag. Concr. Res.* 51 (2) (1999) 87–96.
- [6] N.R. Buenfeld, J.B. Newman, Examination of three methods for studying ion diffusion in cement pastes, mortars and concrete, *Mat. Struct.* 20 (115) (1987) 3–10.
- [7] A.M. Hassanein, G.K. Glass, N.R. Buenfeld, Effect of intermitted cathodic protection on chloride and hydroxyl concentration profiles in reinforced concrete, *Corros. Rev.* 17 (5) (1999) 423–441.
- [8] C. Andrade, M.A. Sanjuán, A. Recuero, O. Rio, Calculation of chloride diffusivity in concrete from migration experiments, in non steady-state conditions, *Cem. Concr. Res.* 24 (7) (1994) 1214–1228.
- [9] D. Baweja, H. Roper, V. Sirivivatnanon, Chloride induced steel corrosion in concrete: Part 1—Corrosion rates, corrosion activity, and attack areas, *ACI Mater. J.* 95 (3) (1998) 207–217.
- [10] T.K.H. Al-Kadhimi, P.F.G. Banfill, S.G. Millard, J.H. Bungey, An accelerated carbonation procedure for studies on concrete, *Adv. Cem. Res.* 8 (30).
- [11] J.O'M. Bockris, A.K.N. Reddy, *Modern Electrochemistry 1—Ionics*, 2nd ed., Plenum, New York, 1998.
- [12] P.C. Kreijger, Inhomogeneity in concrete and its effect on degradation: a review of technology, in: R. Dhir (Ed.), *Conf. Chall. Concr. Constr.*, T. Telford, London, 1990, pp. 32–52.
- [13] H. Brasse, Vorlesungsscript zur Geoelektrik für Studenten mit Geophysik als NebenfachKapitel 2—Gleichstromgeoelektrik, University of Berlin, Berlin, 2001.
- [14] A.J. Bard, L.R. Faulkner, *Electrochemical Methods—Fundamentals and Applications*, Wiley, New York, 1980.
- [15] S. Chatterji, Evidence of variable diffusivity of ions in saturated cementitious materials, *Cem. Concr. Res.* 29 (4) (1999) 595–598.
- [16] W. Breit, Untersuchungen zum kritischen korrosionsauslösenden Chloridgehalt für Stahl in Beton, PhD thesis, Aachen, 1997.
- [17] M. Siegart, B.J. McFarland, J.F. Lyness, A. Abu-Tair, Application of inhibitors to reduce the hydrogen uptake of steel during electrochemical chloride extraction, *Corrosion* 58 (3) (2002) 257–266.
- [18] H.F. Taylor, *Cement Chemistry*, 2nd ed., T. Telford, London, 1998.
- [19] P.F.G. Banfill, Re-alkalisation of carbonated concrete—effect on concrete properties, *Constr. Build. Mater.* 11 (4) (1997) 255–258.
- [20] J.-Z. Zhang, N.R. Buenfeld, Presence and possible implications of a membrane potential in concrete exposed to chloride solution, *Cem. Concr. Res.* 27 (6) (1997) 853–859.
- [21] C. Alonso, C. Andrade, M. Castellote, Processes developed during chloride extraction and re-alkalisation, COST 521 Workshop. Queens University, Belfast, 2000, pp. 297–301.
- [22] J. Mietz, Electrochemical rehabilitation methods for reinforced concrete structures—a state of the art report, *Eur. Fed. Corro. Publ.* 24 (1998) 11.
- [23] J.O'M. Bockris, A.K.N. Reddy, *Modern Electrochemistry 2B—Electrode Processes in Chemistry, Engineering, Biology and Environment Science*, 2nd ed., Plenum, New York, 1998.
- [24] S. Chatterji, M. Kawamura, Electrical double layer, ion transport and reactions in hardened cement paste, *Cem. Concr. Res.* 22 (5) (1992) 774–782.